NASA Technical Memorandum 102555

The Oxidation and Corrosion of ODS Alloys

Carl E. Lowell and Charles A. Barrett
Lewis Research Center
Cleveland, Ohio

June 1990

NASA

THE OXIDATION AND CORROSION OF ODS ALLOYS

Carl E. Lowell and Charles A. Barrett
National Aeronautics and Space Administration
Lewis Research Center
Cleveland, Ohio 44135

SUMMARY

This paper is a review of the oxidation and hot corrosion of high temperature oxide dispersion strengthened (ODS) alloys. It classifies the environmental resistance of such alloys by oxide growth rate, oxide volatility, oxide spalling, and hot corrosion limitations. Also discussed are environmentally resistant coatings for ODS materials. The report concludes that ODS NiCrAl and FeCrAl alloys are highly oxidation and corrosion resistant and can probably be used uncoated.

INTRODUCTION

Oxide dispersion strengthened (ODS) alloys have long been known to have oxidation resistance that is, in general, superior to that of conventional alloys developed for high temperature applications. This gave rise to the expectation that ODS materials could be used at elevated temperatures without a protective coating to prevent excessive oxidation. Such a belief was based on the early oxidation data on thoria dispersion strengthened nickel (TD-Ni) (ref. 1) and thoria dispersion strengthened nichrome (TD-NiCr) measured in isothermal and cyclic, static air tests. Both alloys were developed by DuPont and later Fansteel during the 1960's. This work seemed to indicate that alloys such as TD-NiCr and DS-NiCr (the Sherrit Gordon Incorporated version of the same alloy) had potential for use uncoated at temperatures as high as 1473 K. TD-Ni, on the other hand, even though exhibiting an oxidation rate slightly lower than pure nickel (Wlodek, 1962; Jones and Westerman, 1963; Pettit and Felten, 1964; and Lowell et al., 1972), still oxidized at a rate which was inadequate for use without a protective coating. Much of this early work has been summarized by Wright (1972).

The inherent oxidation resistance of ODS alloys led to their application in a number of materials systems. One of the most widely investigated potential applications was the thermal protection system (TPS) for the space shuttle which was then in its early stages of design (Gilbreath, 1971; and Klingler et al., 1971). Another potential use was the high pressure turbine first stage vanes for the F-101 engine then under development for the B-1 bomber (Stahl, Perkins, and Bailey, 1972). In the 1980's other engine applications were found for these or similar alloys (Singer and Arzt, 1986). It was soon recognized, however, that all such applications, particularly the first two, required not only exposure to cyclic high temperatures, but also exposure to high gas velocities, which could be in excess of Mach 1. Under these conditions chromium oxide (Cr_2O_3) which forms on both TD-NiCr and the DS-NiCr had little chance to perform a protective role due to its volatility at temperatures above 1273 K (Goward, 1970; Scruggs, 1970; Kohl and Stearns, 1970; Giggins and Pettit, 1971; Lowell et al., 1971; Gilbreath, 1971; Sanders and Barrett, 1971; Wallwork and Heo, 1971; and Davis, Graham, and Kvernes, 1971).

The recognition of this major shortcoming led to the accelerated development of thoria dispersion strengthened NiCrAl (TD-NiCrAl) in the mid 1970's. This alloy formed a nonvolatile aluminum oxide (Al_2O_3) scale which was expected to be resistant to high gas velocities. At the same time, protection from hot corrosion was added to the list of requirements which led to dispersion strengthened FeCrAl alloys being developed for such applications in the mid 1970's (Allen and Perkins, 1972). While both the TD-NiCrAl and the Yttria strengthened FeCrAl seemed to have considerable promise in high velocity oxidizing environments, another life limiting criterion came into play--the spalling of the protective Al_2O_3 as a result of thermal expansion mismatch stresses.

The object of this paper is to survey the effects of oxidation and hot corrosion on high temperature ODS alloys and discuss the limitations that the environment imposes on the use of these materials. This survey will be primarily limited to those ODS alloys strengthened by either thoria or yttria and to high temperature effects at 1173 K and above. It will deal with both isothermal and cyclic exposures and especially with high gas velocities, i.e., above Mach 0.2. Also discussed will be coating systems that have been devised to overcome some of the lack of environmental resistance that characterizes some highly alloyed ODS alloy systems, e.g., MA6000E (Gedwill, Glasgow, and Levine, 1982). Models for effects such as volatilization and spalling will be evaluated in the context of dispersion strengthening, with emphasis placed upon the models' ability to predict environmental resistance in a quantifiable fashion.

The first part of this paper will discuss the growth of protective oxides and those ODS materials which are limited by oxide growth kinetics. The effects of oxide volatility will then be examined and discussed in terms of life limitations. This will be followed by an evaluation of the role of scale spalling as a limitation on the use of ODS alloys. The following section will evaluate the effects of hot corrosion; then coatings will be addressed in the context of the peculiar problems that ODS alloys present for their application. Finally, a summary section will attempt to put the environmental effects on ODS alloys into perspective in regard to other material systems for use in high temperature, environmentally active applications.

ALLOYS LIMITED BY OXIDE GROWTH RATES

The kinetics of oxide scale growth were initially elucidated by Wagner (1940) and later expanded by Hauffe (1965). Their work demonstrated that these kinetics were rate limited by the diffusion of anions and/or cations through the oxide scale with the result that the instantaneous growth rate was determined by the diffusion rate of the ions and the thickness of the oxide layer. The growth of oxide scales can therefore be expressed by the following equation:

$$\text{Oxide thickness} = k_{ox}^{1/2} t^{1/2} \qquad (1)$$

where k_{ox} is defined as a growth constant, usually called the parabolic scaling constant as the equation as derived is a parabola, and t is the time. This equation is more commonly expressed as:

$$\frac{\Delta W}{A} = k_p^{1/2} t^{1/2} \tag{2}$$

where $\Delta W/A$ is the specific weight gain usually expressed in milligrams per square centimeter. In this case k_p is the growth constant in terms of weight gain of oxygen.

Assuming that the rate controlling process remains the same during scale growth (i.e., the same scale composition), the temperature (T) dependence of $\ln k_p$ is linear in $1/T$ with an activation energy equal to that of the diffusing species:

$$k_p = k_p^0 \exp\left(\frac{-\Delta E}{RT}\right) \tag{3}$$

An Arrhenius plot for various metals and alloys meeting the above criterion is shown in figure 1, based upon table II. Here data for the most important ODS materials are presented together with several nondispersion strengthened alloys for comparison.

Typical derived kp values for TD-Ni at various temperatures as determined by several investigators particularly Wlodek (1962); Manning, Royster, and Braski (1963); Pettit and Felten (1964); and Lowell, Grisaffe, and Deadmore (1972) are shown in figure 1. While this alloy is a NiO former and the presence of thoria seems to lower the k_p slightly in comparison to pure nickel, the degree of improvement is still not sufficient to allow TD-Ni to be used uncoated at temperatures above 1273 K. Analysis of the remaining data indicates that the alloys with the lowest k_p's are those which form single oxide scales of either Cr_2O_3 or Al_2O_3. Typical of these are TD-NiCr and TD-NiCrAl respectively. While there is some diffusion evidence that a scale composed entirely of nickel chromite or nickel aluminate spinel would have small k_p values, all attempts to form such a scale have failed (Goward, 1970). Even though oxidized TD-NiCrAl scales are often found to have small amounts of nickel aluminate spinel, its generally believed (e.g., Barrett and Lowell, 1975) that the excellent oxidation resistance of this and similar alloys is primarily a result of Al_2O_3 formation containing small amounts of Cr_{3+} ions in solution.

The results of figure 1 demonstrate that, in general, the addition of an oxide dispersoid to an alloy decreases the scale growth rate, e.g., slightly in the case of TD-Ni but by a factor of two or more in the case of TD-NiCr. The mechanism of this rate reduction in TD-NiCr has been studied by several investigators including Giggins and Pettit (1971); Stringer, Wilcox, and Jaffe (1972); and Michaels (1976). While the exact mechanism is still subject to some dispute, clearly the rate reduction is due to a lowering of the rate of ion transport either into or through the scale. In the case of transport through the scale, it has been postulated by Giggins and Pettit (1971) that the dispersed oxide becomes entrapped in the scale reducing diffusion through the scale or alternatively (Michaels, 1976), absorption by the scale of cations from the dispersoid could also reduce diffusion through the scale. Davis, Graham, and Kvernes (1971) suggested that diffusion of chromium through NiCr alloys was decreased by oxide dispersions thus reducing the rate of chromium transport to the metal-scale interface and restricting chromia scale growth. Any of the above mechanisms could account for the observed reductions in oxide

growth rate, but the present authors lean toward the absorption of cations from the dispersoid in the growing scale as the most likely mechanism.

In general, most ODS alloys have good to excellent isothermal oxidation resistance even as compared to coated superalloys (fig. 1). The major exception is TD-Ni. Coatings for improved environmental resistance for use on this alloy have had indifferent success.

ALLOYS LIMITED BY OXIDE VOLATILITY

As discussed in section 2, TD-NiCr is an alloy with sufficient oxidation resistance to allow its use uncoated at temperatures to 1473 K; thus it was considered for use in the TPS of the space shuttle. However, many investigators also recognized that chromia, the protective oxide scale, was volatile in the presence of oxygen (Goward, 1970; Scruggs, 1970; Kohl and Stearns, 1970; Giggins and Pettit, 1971; Lowell et al., 1971; Gilbreath, 1971; Sanders and Barrett, 1971; Wallwork and Hed, 1971; and Davis, Graham, and Kvernes, 1971) which could be a serious problem at the velocities expected for TPS applications. The pertinent chemical reaction was shown to be (Kohl and Stearns, 1970):

$$Cr_2O_3(s) + \frac{3}{2} O_2(g) \rightarrow 2CrO_3(g) \qquad (4)$$

At temperatures below 1473 K in still or slowly moving air, this reaction proceeds at a relatively low rate. However, as the air flow increases, the reaction products can be swept away and the reaction rate can increase to the limiting Langmuir rate (Dushman, 1962). Such losses of chromia can be further aggravated by the presence of water vapor which results in the formation of $Cr_2(OH)_3$ (Kohl and Stearns, 1970) a gaseous species which is even more volatile than CrO_3. Additionally exposure to partial pressures of atomic oxygen at high reentry velocities would even further accelerate chromia vaporization (Fryburg, Kohl, and Stearns, 1972). For any mechanism which drives equation (4) to the right, the net effect has been observed to be that the rate of CrO_3 formation can exceed the rate of formation of Cr_2O_3 and thus protective scale formation is compromised. With the reduction in the rate at which a protective chromia scale forms, scale thickening is diminished and transport across the scale remains high and metal consumption is increased. This effect can be described by:

$$\frac{\Delta W}{A} = k_p^{1/2} t^{1/2} - k_v t \qquad (5)$$

where k_v is the rate of loss of a volatile species. A typical example of such behavior is plotted in figure 2. Plotted in the figure is the measured specific weight change for the case where volatility is minimal in static air. For comparison, specific weight gain curves are also plotted for slowly moving air as well as for high velocity air (>Mach 1). In the latter case the rate of loss can approach that calculated from the Langmuir equation. For the case of slowly moving air the weight change is positive at first, goes through a maximum and ultimately approaches a constant negative rate at which point the oxide scale growth rate is exactly balanced by the loss via oxidative vaporization. For the case of high velocity air the rate of loss is so great that effectively no chromia scale formation can be supported.

A more important measure of the practical implication of the oxidation process is the rate at which metal is consumed. This is plotted in figure 3, for the data used in figure 2, and presents a more graphic demonstration of the effect of volatility. It is evident that the effect of the vapor loss via CrO_3 is to keep the rate of metal consumption at a high, constant value. This is in contrast with alloys whose protective scale is nonvolatile and consequently whose metal consumption rate steadily diminishes with time.

This process of oxidation controlled by volatility has been modeled extensively by Barrett and Pressler (1976) resulting in a computer program called COREST. This program allows one to calculate and accurately predict the weight change and metal consumption from a knowledge of k_p (assuming parabolic growth) and k_v or simply two sets of weight change/time values. The accuracy of this model is primarily determined by the accuracy with which the values of k_p and k_v are known or can be determined. While k_p is primarily a function of temperature and can be measured with considerable precision, k_v is a function of oxygen pressure, flow rate, and geometry as well as temperature and can, in general, be measured only indirectly. The presence of ThO_2 does not affect this k_v value, (Wright, 1972). However, the limiting highest rate can be calculated from the vapor pressure of CrO_3 using the Langmuir equation as shown by Kohl and Stearns (1970). This rate is reached when the gas velocity exceeds about Mach 0.2. Even in slowly moving air the effect of CrO_3 formation on oxidation kinetics becomes noticeable above 1273 K (Lowell et al., 1971). An example of the application of COREST is plotted in figure 4 for TD-NiCr tested in static air. In this figure predicted and measured specific weight change data are plotted and the agreement is seen to be good after the first 10 hr.

The deleterious effects of oxide volatility at high velocities are most easily demonstrated in burner rig tests, e.g., (Lowell and Sanders, 1972; Timbres, Norris, and Clegg, 1972; and Johnston and Ashbrook, 1974), or arc jet facilities, e.g., (Centolanzi et al., 1971; Gilbreath, 1972; Land, Williams, and Perkins, 1972; Tenney, Tang. and Herring, 1974; and Young, Tenney, and Herring, 1975). A burner rig is an apparatus in which material is exposed to combustion gasses exhausted through a convergent nozzle. In burner rig tests gas velocities are commonly between 0.3 and 1.0. Burner rig test results obtained by Lowell and Sanders (1972) on TD-NiCr are shown in figure 5. At short times (<1 hr) metal loss is dominated by the formation and volatilization of a chromia scale. At about 1 hr chromium loss from the metal exceeds the replenishment of chromium via diffusion through metal. This results in the formation of other, less protective oxides--NiO and $NiCr_2O_4$. From that point onward the rate is lower than the initial rate. because these oxides are less volatile, but the rate is still unacceptably large.

The formation of a volatile oxide, CrO_3, prevents the use of TD-NiCr in thick sections, but is even more deleterious for thin sheet (~0.03 cm) applications such as were envisioned for the TPS. Such thin section tests were run in arc jet facilities by the investigators cited above at hypersonic velocities with enhanced degradation results as anticipated. In the arc jet test some atomic oxygen was also present so the results contain effects of both high velocity and enhanced oxidation rate due to the atomic oxygen. Gilbreath (1971) found in oxidizing TD-NiCr at 1373 K that in terms of 10 hr metal recession values obtained in flowing oxygen exceed static oxygen values by a factor of 10 and with atomic oxygen (at unspecified concentrations) present a factor

of 30. As with the burner rig results, within a very short time a chromia scale could not be maintained and the thickness losses were unacceptable even for the relatively short periods (50 hr) needed. In addition to the overall metal loss, the remaining metal was structurally weakened by the presence of Kirkendahl voids resulting from the diffusion of chromium into the scale and the condensation of vacancies around the dispersed oxide particles.

This section has concentrated on TD-NiCr, however, the conclusion that this alloy is not suited to high gas velocity applications at temperatures above 1273 K is equally valid for any ODS alloy, (e.g., MA-754 and IN-853 from table I) which relies upon the formation of a chromia scale for its oxidation protection. Chromia forming alloys can also suffer from enhanced oxidation due to the spalling processes discussed in the next section. However, in high velocity environments the effects of oxidative vaporization are so great that they often mask any effect of spalling, e.g., Lowell and Sanders (1972). Attempts were made by alloying TD-NiCr with 2 to 4 percent manganese to form a scale over the volatile chromia consisting of a $MnCr_2O_4$ spinel Klingler et al. (1971) and Timbres, Norris, and Clegg (1972). While this approach was to some degree successful (Gilbreath, 1972), it was abandoned in favor of the alumina forming TD-NiCrAl as will be discussed in the following section.

ALLOYS LIMITED BY OXIDE SPALLING

TD-NiCrAl was specifically developed to overcome the effects of oxide volatility. In contrast to TD-NiCr which forms chromia as its protective scale, TD-NiCrAl forms an alumina scale which presents no volatility problems at temperatures up to at least 1473 K which is considered to be the useful strength limit for this alloy. In addition neither the presence of water vapor nor atomic oxygen is an important factor in the oxidation process Goward (1970) and Gilbreath (1972). Also, as was demonstrated above, the growth rates of scales on this alloy are among the lowest for any metallic material (fig. 1 and table II). For alloys which form alumina scales the life limiting factor becomes spalling of the protective oxide during cooling from the oxidizing temperature. This includes many of the ODS alloys in table I. Those with compositions of >4 wt % aluminum have alumina as an important scale component; these alloys range from slight variations on TD-NiCrAl like MA-953 to the highly alloyed MA-6000E or MA-755E.

Spalling occurs as a result of thermal expansion mismatch stresses developed between the metal and the oxide (Lowell and Deadmore, 1980). As the alumina grows at temperature, only negligible stresses are developed. Upon cooling the thermal contraction of the metal is much greater than that of the oxide (18×10^{-6} and 10×10^{-6} K, respectively). The result is that the oxide is subjected to stresses that are proportional to the difference in thermal expansion coefficients of the metal and the oxide times the difference between the oxidizing temperature and the temperature to which the material is cooled, i.e.:

$$\sigma \sim \Delta\alpha \times \Delta T \qquad (6)$$

where σ is the stress generated in the scale, $\Delta\alpha$ is difference between the thermal expansion coefficients of the scale and the alloy, and ΔT is the difference between the heating and cooling temperatures. If the stress generated

in the scale exceeds the compressive strength of the oxide, part, or all of the scale will spall. The effect of this process is in some ways analogous to the volatility process. Some, or all of the protective oxide is lost on each cooling cycle and the metal consumption rate may be greatly increased.

The severity of the attack is determined by two major factors. The first is the temperature difference between oxidation and cooling; the greater this difference beyond that needed for the initiation of spalling, the greater the amount of spalling per cycle. This effect is illustrated in figure 6 for TD-NiCrAl as compared to a chromia forming alloy, IN-601 and another alumina forming alloy, FeCrAl. In this figure the specific weight change is shown after 200 1-hr cycles at 1473 K as a function of cooling temperature. These data were obtained in a cyclic furnace test using slowly moving air. Until the difference between the oxidizing temperature and the cooling temperature exceeds about 1100 K the weight change of the TD-NiCrAl is the same as that for an isothermal test. When the difference exceeds 1100 K, spalling was observed and increased as the temperature difference increased. The weight change of the IN-601 showed the same trends, but spalling was observed at smaller values of ΔT, probably the result of the lower compressive strength of chromia. Because of the significantly lower coefficient of thermal expansion of the FeCrAl alloy and consequently reduced stress in the oxide, no spalling was observed even with a ΔT of 1400 K.

The second factor affecting the severity of spallation is the adherence of the scale to the alloy. If the oxide is strongly adherent, fracture will occur within the scale; if the oxide is weakly adherent, fracture will take place at the metal/oxide interface with much more serious consequences. The resultant exposure of bare metal on the next heating cycle will cause a greatly accelerated metal consumption rate. The effects of the two types of spalling are shown in figure 7 from Barrett, 1988) for stoichiometric beta nickel aluminide with and without an addition of 0.1 at % zirconium. Here cyclic oxidation test results are plotted for the alloy without zirconium, which does spall to bare metal, and the aluminide with zirconium, which spalls within the oxide. The former displays a negative weight change almost from the beginning while the latter has a positive weight change throughout the duration of the test only a modest weight loss.

The mechanism of oxide adherence or nonadherence has been the subject of a very large number of investigations. The model which seems to explain most, but perhaps not all of the observations, is that of Smeggil (1986) and Smialek (1987). Both propose that nonadherent alumina scales result from segregation of sulfur at the oxide/metal interface resulting in the disruption of the oxide/metal bond. It has been long known that small amounts of active element additions such as yttrium, zirconium and silicon were effective in promoting adherence between the oxide and the metal. Smialek proposes and appears to have convincing evidence that the function of these additions is to effectively prevent trace sulfur impurities from segregating at the metal/oxide interface. This is accomplished either by chemical combination of the active element and the sulfur, or a reduction of the amount of diffusion of sulfur to the surface of the metal.

The additions of oxide dispersions also are known to have a beneficial effect on oxide adherence. While the mechanism is not established, and it is

difficult to understand how the oxide particles prevent the sulfur from reaching the oxide/metal interface, the fact remains that alumina scales on TD-NiCrAl are adherent and do spall primarily within the scale whether yttrium is present in the alloy or not.

Because of the analogy of the accelerated attack of the spalling process to that of oxide volatility, the first attempts at modeling this attack used a CORREST base (Barrett and Pressler, (1975)). Equation (3) was replaced by:

$$\frac{\Delta W}{A} = k_1^{1/2} t^{1/2} - k_2 t \qquad (7)$$

where k_1 was assumed to be a measure of scale growth analogous to k_p and k_2 was an empirical spalling constant, analogous to k_v. In practice, specific weight gain data is fit by multiple linear regression to obtain estimates of k_1 and k_2. k_1 and k_2 were then combined into one value, K_a, which was shown to be an indication the degree of susceptibility to cyclic oxidation.

While this model has been successfully applied to a number of studies aimed at ranking alloys (see particularly Barrett and Lowell (1977) and subsequent reports Barrett and Lowell (1978); Barrett, Khan, and Lowell (1981); and Barrett and Lowell (1982)) it was recognized that its empirical nature severely limited its predictive utility. The use of this type of equation assumes that the amount of spall per cycle is a constant, clearly an unwarranted assumption with the possible exception of systems in which the oxide spalls completely on every cycle. Thus the concept that k_2 represents a constant spall rate, which has no physical significance, is the major flaw in this approach.

As an alternative approach, the COSP model was developed (Lowell, Smialek, and Barrett, (1983); and Lowell et al. (1988)). It makes two basic assumptions: (1) the growth of an oxide scale during each heating cycle is determined by the amount of oxide on the material at the start of the cycle and, (2) the amount of oxide spalled upon cooling from each heating cycle is proportional to the total amount of oxide on the material at the end of the heating cycle. Inputs to the model are the growth kinetics of the scale and an expression for the dependence of spalling on scale thickness. The latter has been experimentally determined for alumina and chromia scales as shown in figure 8.

Using the data of figure 8, the COSP model has been successfully used to predict cyclic oxidation response by utilizing measurements made from isothermal tests (Lowell, Smialek, and Barrett, 1983). An example of this application is shown in figure 9 which plots cyclic test experimental specific weight change data for TD-NiCrAl. Also plotted are predictions from the COSP model; the agreement is excellent. The major advantages of this model are twofold. By doing one isothermal measurement, one can predict accurately the cyclic oxidation behavior of an alloy for any duration of heating cycle. Equally important is that the model allows calculation of the metal[1] consumed during thermal cycling, a determination hitherto only possible by destruction of the sample. An example of the results of this type of calculation is shown in figure 10.

---

[1]CORREST also computes the specific weight of metal consumed with time (i.e., W_m). If the k_2 value derived for CORREST is quite small the W_m values derived by CORREST and COSP may not differ significantly.

alloys and as well as their coatings. Figure 11 (Lowell, Deadmore, and Whittenberger, 1982) plots burner rig weight change data for several Ni-base ODS alloys which are Al_2O_3 formers similar to TD-NiCrAl in concept as well as an Fe-base ODS alloy, MA-956. For comparison, data for a MCrAlY coated superalloy, also an alumina former is plotted. Especially good performance was obtained for the ODS FeCrAl which showed virtually no attack throughout the entire test. This result was probably due to the fact that the thermal expansion of iron base materials is significantly lower than that of their nickel base equivalents (Deadmore and Lowell 1977). This fact means that the thermal expansion mismatch stresses are considerably less and therefore spalling is substantially reduced (see above and fig. 6). Indeed, ODS FeCrAl is one of the best cyclic oxidation resistant materials measured in this type of test. At the other extreme, figure 11 shows the catastrophic weight loss for TD-NiCr after only a few cycles.

To sum up this section, ODS alloys, which form an alumina protective scale, are excellent in cyclic oxidation as well as in high gas velocity tests. They are therefore able to be used uncoated in most types of oxidation environments at temperatures approaching 1200 °C.

ALLOYS LIMITED BY HOT CORROSION

Hot corrosion is a term usually applied to accelerated oxidation attack which occurs at temperatures where a molten alkali salt is present on the surface of a material, typically ~1173 K. This corrosion process has been delineated for chromia and alumina forming turbine alloys by Fryburg and his coworkers at NASA Lewis (Fryburg et al., 1982; and Fryburg, Kohl, and Stearns, 1984). In the operation of a gas turbine engine the molten salt results from the ingestion of airborne sodium chloride or other alkali salts into the combustor where the salts react with sulfur, which is present at low concentrations in the fuel. This reaction results in the formation of sulfates which condense on the airfoils of the turbine. The molten sulfates flux the protective oxide scale leading to catastrophic attack; in extreme cases, such as can be sometimes found in marine turbines, failure can occur in a few hours.

An excellent simulation of this attack is the burner rig test. Sodium chloride or synthetic sea salt can be injected into the combustor of the burner rig continuously as a water solution. The chloride reacts with the sulfur in the jet fuel used to form sodium sulfate which condenses on the samples after exiting the nozzle, simulating the turbine engine process. The severity of the test can be controlled by the level of salt injection and the temperature. These tests are usually run at the parts per million level of sodium in the air. The temperature most often used in these tests is 1173 K so that the samples are above the melting point of the sulfate (1156 K) but below the dew point (~1300 K at atmospheric pressure).

Hot Corrosion tests have been performed on both chromia and alumina forming ODS alloys. Long time corrosion studies comparing various ODS alloys near 1173 K in burner rig testing have been reported by Lowell and Deadmore, 1977; Benn, 1977; Huber, 1978; Sanford, 1979; Weber, 1980; Glasgow and Santoro, 1982; Huber, 1983; and Kane, 1983. A plot comparing several ODS alloys with IN-792 and MCrAlY coated MAR-M200 is shown in figure 12. Plotted are weight change data for a burner rig hot corrosion test performed at 1173 K on several ODS

alloys as compared to a nickel base superalloy reputed to have reasonably good resistance to hot corrosion (IN-792). All of the ODS alloys were alumina formers and fared quite well compared to IN-792. The two alloys with Ta additions failed (>10 mm/cm^2 loss) earlier than those without Ta and the ODS FeCrAl survived the entire test without any evidence of accelerated attack. These results suggest that as long as the alumina scale remains intact hot corrosion in minimized; the alloy with the least susceptibility to spalling, MA-956 (ODS FeCrAl) showed the least attack. In fact the micrographs taken at the end of the test and shown in figure 13 indicate that there was no attack at all on this alloy. It seems likely that the early failure of the alloys with Ta additions was due to a disruption of the alumina scale induced by inclusion of Ta into the oxide.

Another alloy comparison study by Huber (1978) showed that yttria dispersion strengthened IN-738 had better hot corrosion resistance than IN-738 without the yttria. Kane (1973) tested several alloys and found that MA-956 had by far the greatest resistance to hot corrosion in comparison to a wide range of ODS and conventional alloys.

The results of the tests described indicate that alumina forming ODS alloys and especially the FeCrAl's (e.g., MA-956) can be used uncoated in even the most aggressive hot corrosion environments. However, it must be pointed out that there may be conditions of extreme temperature excursions where the alumina scale might be broached allowing excessive corrosion to occur.

COATINGS FOR ODS ALLOYS

As pointed out earlier, there are some ODS alloys with otherwise attractive properties that cannot be used in aggressive environments without the application of an environmentally resistant coating system. TD-Ni, TD-NiCr and MA6000E all have been shown (see above) to have insufficient resistance to environmental attack. All have been the subjects of coating attempts.

The two most common types of coatings used to resist oxidation and hot corrosion are (1) diffusion coatings usually applied by a pack cementation process and (2) overlay coatings applied either by physical vapor deposition (PVD) or plasma spraying (PS). Of the two general types overlay coating are generally preferred. This is due to the fact that they result in a coating which has much less interdiffusion between the coating and the substrate. The compositions of overlay coatings that can be applied are generally more resistant to environmental attack, especially hot corrosion. The most common type of PVD or PS overlay coating compositions are the MCrAlY where M is nickel and/or cobalt and the role of the yttrium is to promote scale adhesion.

Overlay coatings have been successfully applied to nickel and cobalt base superalloys. The lives of such coatings on superalloys are limited by the rate at which aluminum in the coating is lost by diffusion into the substrate and by scale formation. Such coating systems have been successfully used for tens of thousands of hours and are bill-of-materials for high temperature components in commercial aeropropulsion turbines. However, the use of these systems on ODS alloys has been hampered by porosity formation resulting from interdiffusion between the MCrAlY coating and the ODS substrate. While the formation of porosity also occurs in coated superalloys, it is present to a considerably

thousands of hours and are bill-of-materials for high temperature components in commercial aeropropulsion turbines. However, the use of these systems on ODS alloys has been hampered by porosity formation resulting from interdiffusion between the MCrAlY coating and the ODS substrate. While the formation of porosity also occurs in coated superalloys, it is present to a considerably lesser degree (Glasgow and Santoro, 1981). This effect can be tolerated until sufficient porosity forms to cause exfoliation of the coating from the substrate alloy. The microstructure shown in figure 14 demonstrates this effect which is often observed after only a few hundred hours.

Fortunately, considerable progress has been made in the application of overlay coatings on the MA6000E (Glasgow and Santoro, 1981). While these results hold out hope that ODS alloys can successfully be protected from environmental attack by the use properly designed coating systems, further development and more extensive testing are needed before one can have confidence that coatings can be produced with sufficient reliability that they can be used in commercial applications.

CONCLUDING REMARKS

Regardless of whether the environmental attack is one of oxidation or hot corrosion, isothermal or cyclic, or still air or high velocity air, some ODS alloys can find use uncoated. The alloys with greatest resistance are those which form a protective alumina scale, primarily the NiCrAl and FeCrAl alloys with the latter having the most resistance to environmental resistance attack. Indeed the resistance of ODS FeCrAl (MA-956) is equivalent or better than the best coating alloys currently available. Therefore, the use of these alloys in high temperature applications is not limited by either oxidation or hot corrosion at temperatures up to 1473 K. The same cannot be said for nonalumina forming ODS alloys such as TD-Ni, TD-NiCr, or MA6000E. In order for these alloys to be used under severe conditions, coatings tailored to the peculiar requirements of these alloys will have to be developed.

In sum, ODS alloys, as a class, have better environmental resistance than similar alloys without dispersion strengthening. From an environmental durability standpoint ODS have a great deal to recommend them.

REFERENCES

Allen, R.E.; and Perkins, R.J. (1972) Strengthening of FeCrAlY Oxidation Resistant Alloys. Aircraft Engine Group, General Electric Company (Avail. NTIS, AD-902087L).

Barrett, C.A. (1988) Effect of 0.1 at % Zirconium on the Cyclic Oxidation Resistance of β-NiAl. Oxid. Met., vol. 30, nos. 5/6, pp. 361-390.

Barrett, C.A.; and Evans, E.B. (1973) Cyclic Oxidation Evaluation - Approaching Application Conditions. NASA TMX-68252.

Barrett, C.A.; Johnston, J.R.; and Sanders, W.A. (1978) Static and Dynamic Cyclic Oxidation of 12 Nickel-, Cobalt-, and Iron-Base High-Temperature Alloys. Oxid. Met., vol. 12, no. 4, pp. 343-377.

Barrett, C.A.; Khan, A.S.; and Lowell, C.E. (1981) The Effect of Zirconium on the Cyclic Oxidation of NiCrAl Alloys. J. Electrochem. Soc., vol. 128, no. 1, Jan. pp. 25-32.

Barrett, C.A.; and Lowell, C.E. (1975) Comparison of Isothermal and Cyclic Oxidation Behavior of Twenty-Five Commercial Sheet Alloys at 1150 °C. Oxid. Met., vol. 9, no. 4, pp. 307-355.

Barrett, C.A.; and Lowell, C.E. (1977) Resistance of Ni-Cr-Al Alloys to Cyclic Oxidation at 1100 and 1200 °C. Oxid. Met., vol. 11, no. 4, pp. 199-223.

Barrett, C.A.; and Lowell, C.E. (1982) High Temperature Cyclic Oxidation Furnace Testing at NASA Lewis Research Center. J. Test. Eval., vol. 10, pp. 273-278.

Barrett, C.A.; and Presler, A.F. (1976) COREST: A Fortran Computer Program to Analyze Paralinear Oxidation Behavior and Its Application to Chromic Oxide Forming Alloys. NASA TN D-8132.

Benn, R.C. (1977) Quaternary and Higher Volumes Alloy Additions to Oxide Dispersion Strengthened High Volume Fraction Gamma Prime Ni-Cr-Al Alloys Made by Mechanical Alloying. NADC-76204-30. (Avail. NTIS, AD-A053779).

Centolanzi, F.J., et al. (1971) Arc Jet Tests of Metallic TPS Materials. NASA TM X-62092.

Davis, H.H.; Graham, H.C.; and Kvernes, I.A. (1971) Oxidation Behavior of Ni-Cr-1ThO_2 Alloys at 1000 and 1200 °C. Oxid. Met., vol. 3, no. 5, p. 431.

Deadmore, D.L.; Lowell, C.E.; and Santoro, G.J. (1975) High Gas Velocity Oxidation and Hot Corrosion Testing of Oxide Dispersion-Strengthened Nickel-Base Alloys. NASA TM X-71835.

Dushman, S. (1962) Scientific Foundations of Vacuum Technique. 2nd Ed., John Wiley & Sons, Inc., New York.

Fryburg, G.C., et al. (1982) Chemical Reactions Involved in the Initiation of Hot Corrosion of B-1900 and NASA-TRW VIA. J. Electrochem. Soc., vol. 129, no. 3, pp. 571-585.

Fryburg, G.C.; Kohl, F.J.; and Stearns, C.A. (1972) Enhanced Oxidative Vaporization Of Cr_2O_3 and Chromium by Oxygen Atoms. J. Electrochem. Soc., vol. 121, no. 7, pp. 952-959.

Fryburg, G.C.; Kohl, F.J.; and Stearns, C.A. (1984) Chemical Reactions Involved in the Initiation of Hot Corrosion of IN-738. J. Electrochem. Soc., vol. 131, no. 12, pp. 2985-2997.

Gedwill, M.A.; Glasgow, T.K.; and Levine, S.R. (1982) A New Diffusion-Inhibited Oxidation-Resistant Coating for Superalloys. Thin Solid Films, vol. 95, pp. 65-72.

Giggins, C.S.; and Pettit, F.S. (1971) The Oxidation of TD NiC (Ni-20Cr-2 vol pct ThO_2) Between 900° and 1200 °C. Met. Trans, vol. 2, no. 4, pp. 1071-1078.

Gilbreath, W.P. (1971) Preliminary Studies of the Oxidation of TD Ni-20Cr in Static, Flowing, and Dissociated Oxygen at 1100 °C and 130 Nm^{-2}. NASA TM X-62064.

Gilbreath, W.P. (1972) The Degradation of Space Shuttle TPS Metals in Dissociated Oxygen. AIAA Paper 72-262.

Glasgow, T.K.; and Santoro, G.J. (1981) Oxidation and Hot Corrosion of Coated and Bare Oxide Dispersion Strengthened Superalloy MA-755E. Oxid. Met., vol. 15:, nos. 3-4, pp. 251-276.

Goncel, O.T.; Whittle, D.P.; and Stringer, J. (1981) The Oxidation Behavior of Fe-Cr Alloys Containing HfO2-Dispersed Phase. Oxid. Met., vol. 15, nos. 3-4, pp. 287-295.

Goward, G.W. (1970) Current Research on the Surface Protection of Superalloys for Gas Turbine Engines. J. Met., vol. 22, no. 10, pp. 31-39.

Hauffe, K. (1965) Oxidation of Metals. Plenum Press, New York.

Huber, P. (1978) Corrosion Rig Tests for Evaluation of Gas Turbine Materials and the Determination of the Influence of Physical and Chemical Parameters on the Corrosion Behavior of Nickel- and Cobalt-Base Alloys, High Temperature Alloys For Gas Turbines. D. Coutsouradis, et al., eds., Applied Science Publishers, Ltd., London, pp. 251-258.

Huber, P. (1983) Hot Corrosion Testing of Oxide Dispersion Strengthened Nickel Base Alloys. Frontiers of High Temperature Materials II, J.S. Benjamin and R.C. Benn, eds., Inco Alloys Int., Huntington, WV, pp. 317-326.

Johnston, J.R.; and Ashbrook, R.L. (1974) Effect of Cyclic Conditions on the Dynamic Oxidation of Gas Turbine Superalloys. NASA TN D-7614.

Jones, D.A.; and Westerman, R.E. (1963) Oxidation of a Nickel -2% ThO_2 Alloy and the Logarithmic Rate Law of Oxidation. Rept. HW-79350, General Electric Co., Hanford Atomic Products Operation, Richland, WA (Avail. NTIS).

Kane, R.H. (1983) Some Aspects of High Temperature Corrosion of Oxide Dispersion Strengthened Alloys. Frontiers of High Temperature Materials II. J.S. Benjamin, and R.C. Benn, eds., Inco Alloys Int., Huntington, WV, pp. 392-418.

Khan, A.S.; Lowell, C.E.; and Barrett, C.A. (1980) The Effect of Zirconium on the Isothermal Oxidation of Nominal Ni-14Cr-24Al Alloys. J. Electrochem. Soc., vol. 127, no. 3, pp. 670-679.

Klingler, L.J.; et al. (1971) Development of Dispersion Strengthened Nickel-Chromium Alloy (Ni-Cr-ThO2) Sheet for Space Shuttle Vehicles. NASA CR-120796.

Kohl, F.J.; and Stearns, C.A. (1970) Vaporization of Chromium Oxides from the Surface of TD-NiCr Under Oxidizing Conditions. NASA TM X-52879.

Land, D.W.; Williams, R.R.; and Rinehart, W.A. (1972) Testing Superalloys at 2000 (1367) and 2200 °F (1478 K) in a Mach 4.6 Airstream. (MDC-Q0499, McDonnell Corp.; NASA Contract NAS3-14666-H) NASA CR-120913.

Lowell, C.E.; et al. (1971) Oxidation of Ni-20Cr-2ThO_2 and Ni-30Cr-1.5Si at 800 °C, 1000 °C, and 1200 °C. NASA TND-6290.

Lowell, C.E.; et al. (1988) COSP-A Computer Program to Model Cyclic Oxidation.

Lowell, C.E.; and Deadmore, D.L. (1977) High Velocity Oxidation and Hot Corrosion Resistance of Some ODS Alloys. NASA TM X-73656.

Lowell, C.E.; and Deadmore, D.L. (1980) The Role of Thermal Shock in Cyclic Oxidation. Oxid. Met., vol. 14, no. 4, pp. 325-336.

Lowell, C.E.; Deadmore, D.L.; and Whittenberger, J.D. (1982) Long-Term High-Velocity Oxidation and Hot Corrosion Testing of Several NiCrAl and FeCrAl Base Oxide Dispersion Strengthened Alloys. Oxid. Met., vol. 17, nos. 3-4, pp. 205-221.

Lowell, C.E.; Grisaffe, S.J.; and Deadmore, D.L. (1972) Oxidation of TD Nickel at 1050 and 1200 °C as Compared to Three Grades of Nickel of Different Purity. Oxid. Met., vol. 4, no. 2, pp. 91-111.

Lowell, C.E.; and Sanders, W.A. (1972) Mach 1 Oxidation of Thoriated Nickel Chromium at 1204 °C (2200 °F). Oxid. Met., vol. 5, no. 3, pp. 221-239.

Lowell, C.E., Smialek, J.L. ; and Barrett, C.A. (1983) Cyclic Oxidation of Superalloys. High Temperature Corrosion, R.A. Rapp, ed., National Association of Corrosion Engineers, pp. 219-226.

Manning, C.R.; Royster, D.M.; and Braski, D.N. (1963) An Investigation of a New Nickel Alloy Strengthened by Dispersed Thoria. NASA TN D-1944.

Michels, H.T. (1976) The Effect of Dispersed Reactive Metal Oxides on the Oxidation Resistance of Nickel-20 Wt Pct Chromium Alloys. Metall. Trans. A, vol. 7, no. 3, pp. 379-388.

Michels, H.T. (1977) The Effect of Dispersed Oxides on the Oxidation Behavior of Al- and Ti- Containing Ni-20 Pct Cr Alloys. Metall. Trans. A, vol. 8, no. 2, pp. 273-278.

Michels, H.T. (1978) The Oxidation of Oxide Dispersion Strengthened Ni-15Cr-5Al Alloys. Metall. Trans. A, vol. 9, no. 6, pp. 873-878.

Nagai, H.; and Okabayashi, M. (1981) High-Temperature Oxidation of Ni-20Cr Alloys with Dispersion of Various Reactive Metal Oxides. Trans. Jpn. Inst. Met., vol. 22, no. 2, pp. 101-108.

Peck, J.V.; Bublick, A.V.; and Berkley, S.G. (1972) Development of Production Manufacturing Techniques for Application of Protective Coatings to Thoria Dispersion Strengthened Alloys. AFML-TR-72-86 (Avail. NTIS, AD-901796L).

Pettit, F.S.; and Felten, E.J. (1964) The Oxidation of Ni-2ThO2 Between 900° and 1400 °C, J. Electrochem. Soc., vol. 111, no. 2, pp. 135-139.

Ramanarayanan, T.A.; Raghavan, M.; and Petkovic-Luton, R. (1984) The Characteristics of Alumina Scales Formed on Fe-Based Yttria-Dispersed Alloys. J. Electrochem. Soc., vol. 131, no. 4, pp. 923-931.

Rhee, S.K.; and Spencer, A.R. (1971) Cyclic Oxidation of TD-Nickel. Met. Trans., vol. 2, no. 8, pp. 2285-2287.

Rosenberg, R.A. (1964) Oxidation of Rene 41 and Thoriated Nickel Wires Between 1600 F and 2000 °F. GAW/MECH/64-18 (Avail. NTIS, AD-610241).

Saegusa, F. (1966) Oxidation of Nickel and Nickel-Cobalt Dispersion Strengthened Alloys. WVT-6602 (Avail. NTIS, AD-482191).

Sanders, W.A.; and Barrett, C.A. (1971) Oxidation Screening at 1204 °C (2200 °F) of Candidate Alloys for the Space Shuttle Thermal Protection System. NASA TM X-67864.

Santoro, G.J. (1979) Hot Corrosion of Four Superalloys: HA-188, S-57, IN-617, and TD-NiCrAl. Oxid. Met., vol. 13, no. 5, pp. 405-435.

Scruggs, D.M. (1970) Oxidation and Agglomeration Resistance of Thin Gage Dispersion Strengthened Alloys. NASA CR-111807.

Singer, R.F.; and Arzt, E. (1986) Structure Processing and Properties of ODS Superalloys. High Temperature Alloys for Gas Turbines and Other Applications, Part 1, W. Betz, et al., eds., D. Reidel Publishing Co., 1986, pp. 97-126.

Smeggil, J.G. (1987) Some Comments on the Role of Yttrium in Protective Oxide Scale Adherence. Mater. Sci. Eng., vol. 87, pp. 261-265.

Smialek, J.L. (1988) The Effect of Sulfur and Zirconium Co-Doping on the Oxidation of NiCrAl. NASA TM-100209.

Stahl, J.A.; Perkins, R.J.; and Bailey, P.G. (1979) Low Cost Process for Manufacturing of Oxide Dispersion Strengthened (ODS) Turbine Nozzle Components. Air Force Materials Laboratories, TR-AFML-TR-79-4163 (Avail. NTIS, AD-A088019).

Stringer, J.; Wilcox, B.A.; and Jaffe, R.I. (1972) The High-Temperature Oxidation of Nickel-20 wt. % Chromium Alloys Containing Dispersed Oxide Phases. Oxid. Met., vol. 5, no. 1, pp. 11-47.

Tenney, D.R.; Young, C.T.; and Herring, H.W. (1974) Oxidation Behavior of TD-NiCr in a Dynamic High Temperature Environment. Met. Trans. 5, no. 5, pp. 1001-1012.

Timbres, D.H.; et al. (1973) The Development of an Improved Oxidation-Resistant Dispersion Strengthened Nickel-Chromium Alloy. Modern Developments in Powder-Metallurgy, Vol. 8, Ferrous P/M & Special Materials, H.H. Hausner and W.E. Smith, eds., American Powder Metallurgy Institute, Princeton, NJ, pp. 391-418.

Wallwork, G.R.; and Hed, A.Z. (1971) The Oxidation of Ni-20 wt. % Cr-ThO2. Oxid. Met., vol. 3, no. 3, pp. 229-241.

Weber, J.H. (1980) High Temperature Oxide Dispersion Strengthened Alloys. SAMPE Q., vol. 11, no. 4, pp. 35-42.

Wlodek, S.T. (1962) The Oxidation of Ni-2 percent ThO_2. General Electric Co., Rep. R62 FPD 140.

Wright, I.G. (1972) Oxidation of Iron-, Nickel-, and Cobalt-Base Alloys. MCIC-72-07, Metals and Ceramics Information Center, Battelle Columbus Labs., Columbus, OH (Avail. NTIS, AD-745473).

Wright, I.G.; and Wilcox, B.A. (1974) The Oxidation of Fe-Cr Alloys Containing Oxide Dispersion or Reactive Metal Additions. Oxid. Met., vol. 8, no. 5, pp. 283-301.

Young, C.T.; Tenney, D.R.; and Herring, H.W. (1975) Dynamic Oxidation Behavior of TD-NiCr Alloy with Different Surface Pretreatments. Metall. Trans. A, vol. 6, no. 12, pp. 2253-2265.

TABLE I. - COMPOSITION OF ODS ALLOYS IN WEIGHT PERCENT EXCEPT WHERE NOTED

Alloy	Fe	Ni	Cr	Al	Ti	Co	Mo	W	Ta	Nb	C	B	Zr	Dispersoid(s)
TD-Ni	0.05	Bal.	0.05	---	0.05	0.2	---	---	---	---	-----	-----	-----	1.8 to 2.6 ThO_2
TD-NiCr	-----	↓	20	---	-----	---	---	---	---	---	-----	-----	-----	2.0 ThO_2
DS-NiCr	-----		20	---	-----	---	---	---	---	---	-----	-----	-----	↓
TD-NiCrFe	18		20	---	-----	---	---	---	---	---	-----	-----	-----	
TD-NiCrAl	-----		16	5	-----	---	---	---	---	---	-----	-----	-----	
TD-NiCrAlY	-----		15	5	-----	---	---	---	---	---	-----	-----	-----	
DS-IN-738	-----	Bal.	16	3.4	3.4	8.5	1.8	2.6	1.8	0.9	0.17	0.01	0.1	1.5 Y_2O_3
IN-853	-----	↓	20	1.5	2.5	---	---	---	---	---	-----	-----	-----	2.5 vol % Y_2O_3
MA-754	1		20	0.3	0.5	---	---	---	---	---	0.05	-----	-----	0.6 Y_2O_3
MA-755	-----		15	4.5	3	---	3.5	5.5	2.5	---	-----	-----	-----	1.1 Y_2O_3
MA-953	35		21	5.5	0.5	---	---	---	---	---	-----	-----	-----	0.3 La_2O_3
MA-956	Bal.	0.4	18.9	4.4	0.5	---	---	---	---	---	0.02	-----	-----	0.6 Y_2O_3
MA-6000	-----	Bal.	15	4.5	2.5	---	2	4	2	---	0.05	0.01	0.15	1.1 Y_2O_3
AT-259/HA-8077	-----	Bal.	15.7	4.2	-----	---	---	---	---	---	0.06	-----	-----	1.6 Y_2O_3
AT-264	-----	↓	15.7	4.5	-----	1	---	---	---	---	0.05	-----	-----	1.5 Y_2O_3
AT-265	-----		16	4.7	-----	0.7	---	---	1.7	---	0.05	-----	-----	1.5 Y_2O_3
AT-266	-----		15.9	4.9	-----	0.4	---	---	1.2	---	0.05	-----	-----	1.5 Y_2O_3

TABLE II. - PARABOLIC SCALING CONSTANT, kp FOR VARIOUS Ni OR Fe-BASED ODS ALLOYS

[Other studies with Fe-Cr or Ni-Cr plus dispersoids (e.g., ThO_2, Y_2O_3, etc.) show complex kinetics above 1273 K due to vaporization of the chromia and the effect of the dispersoid in the chromia. The curves are approximately paralinear with rate constants difficult to derive. Any kp listed for this type of alloy is somewhat questionable. Many investigations just show the range of specific weight change/time data.]

Alloys	Temperature, K	kp, $(mg/cm^2)^2/hr$	Reference
TD-Ni	1255	1.29×10^{-1}	Wlodek - 1962
	1366	1.02	
	1477	5.20	
TD-Ni	1273	2.56×10^{-1}	Jones and Westerman - 1963
TD-Ni	1255	4.28×10^{-2}	Manning, Royster, and Braski - 1963
	1366	1.44	
	1477	5.76	
	1589	19.22	
TD-Ni	1273	2.20×10^{-1}	Pettit - 1964
	1373	1.25	
	1473	2.78	
	1473	6.83	
	1573	13.73	
	1673	26.27	
TD-Ni	1255	3.84×10^{-1}	Rosenberg - 1964
	1366	1.44	
Ni+Al_2O_3	1273	1.00	Saegusa - 1966
	1373	3.51	
TD-NiCr	1373	1.51×10^{-2}	Goward - 1970
TD-Ni	1255	7.09×10^{-1}	Scruggs - 1970
	1366	3.33	
TD-NiCr	1273	5.76×10^{-3}	Giggins and Pettit - 1971
	1273	8.99×10^{-3}	
	1373	7.91×10^{-3}	
	1373	1.22×10^{-2}	
	1473	4.68×10^{-2}	
	1473	5.04×10^{-2}	
TD-Ni	1255	1.63×10^{-1}	Rhee and Spencer - 1971
	1366	1.56	
TD-Ni	1323	3.90×10^{-1}	Lowell, Grisaffe, and Deadmore - 1972
	1477	2.70	
TD-Ni	1366	4.90×10^{-1}	Peck, Bublick, and Berkley - 1972
	1477	10.89	
	1589	19.36	
Fe-16Cr-3 va %Y_2O_3	1373	2.52×10^{-1}	Wright and Wilcox - 1974
TD-Ni	1423	1.35	Barrett and Lowell - 1975
TD-NiCr	1423	6.8×10^{-3}	
TD-NiCrFe	1423	6.3×10^{-3}	
TD-NiCrAlY	1423	1.28×10^{-2}	
Ni-20Cr-0.04La_2O_3-0.04Y_2O_3	1273	1.19×10^{-3}	Michels - 1976
	1373	1.40×10^{-2}	
	1473	1.58×10^{-2}	
Ni-20Cr-0.02La_2O_3	1273	3.60×10^{-3}	
	1373	6.12×10^{-3}	
	1473	9.35×10^{-2}	
Ni-20Cr-1.2Li_2O	1273	2.30×10^{-2}	
	1373	3.96×10^{-2}	
	1473	3.96×10^{-1}	
Ni-20Cr-0.5Al-.5Ti-1.3Y_2O_3	1273	5.29×10^{-3}	Michels - 1977
	1373	4.89×10^{-2}	
	1473	2.82×10^{-1}	
Ni-15Cr-5Al-1.1%Y_2O_3	1273	5.29×10^{-3}	Michels - 1978
	1373	4.89×10^{-2}	
	1473	2.79×10^{-2}	
Fe-14Cr-1 H_f (int. ox.)	1273	3.35×10^{-3}	Goncel, Whittle and Stringer - 1981
	1373	1.19×10^{-2}	
Fe-18Cr-1 H_f (int. ox.)	1273	1.58×10^{-3}	
	1373	8.09×10^{-3}	
Ni-20Cr-0.7Cr_2O_3	1373	3.96×10^{-1}	Nagai and Okabayashi - 1981
	1473	9.39×10^{-1}	
Ni-20Cr-0.7SiO_2	1373	2.96×10^{-1}	
	1473	5.79×10^{-1}	
Ni-20Cr-0.7Al_2O_3	1373	1.45×10^{-1}	
	1473	2.46×10^{-1}	
Ni-20Cr-0.7La_2O_3	1373	8.88×10^{-3}	
	1473	2.09×10^{-2}	
Ni-20Cr-0.7Y_2O_3	1373	5.65×10^{-2}	
	1473	9.64×10^{-2}	
MA-956	1273	1.77×10^{-4}	Ramanarayanan, Raghavan, and Petkovic-Luton - 1984
	1323	7.07×10^{-4}	
	1373	2.56×10^{-3}	
	1473	2.57×10^{-2}	
TD-NiCrAl	1473	2.00×10^{-2}	Unpublished - NASA Lewis data

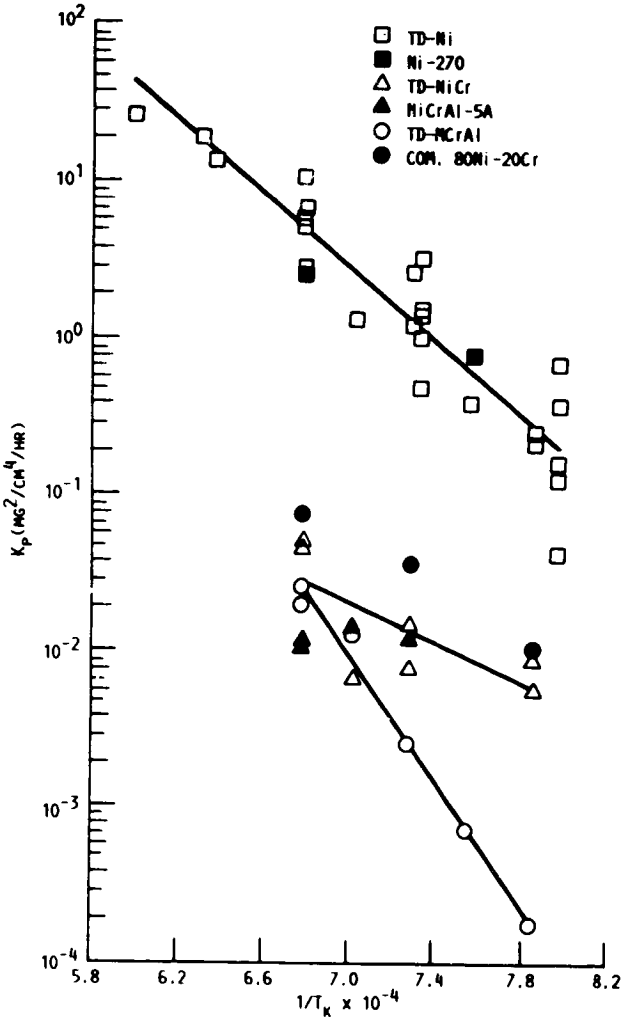

FIGURE 1. - PARABOLIC SCALING CONSTANT AS A FUNCTION OF INVERSE TEMPERATURE OF SELECTED ODS ALLOYS AS TAKEN FROM TABLE 2. FOLLOWS BARRETT AND LOWELL (1975), FIG.7. ALSO PLOTTED ARE DATA FOR PURE NICKEL, Ni-270 (LOWELL, DEADMORE AND GRISAFFE, 1971), A COMMERCIAL Ni-20Cr ALLOY (MICHELS, 1976) AND AN EXPERIMENTAL NiCrAl ALLOY, 5A (KHAN, LOWELL, AND BARRETT, 1980).

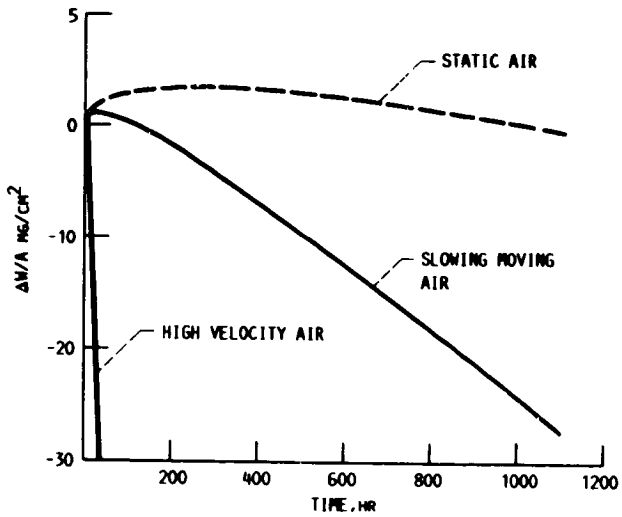

FIGURE 2. - SPECIFIC WEIGHT CHANGE CALCULATED BY PARA-LINEAR ANALYSIS (COREST) FOR Cr_2O_3 FORMING ALLOY, Ni-40Cr AT 1473 K IN STATIC AIR, SLOWLY MOVING AIR AND HIGH VELOCITY AIR.

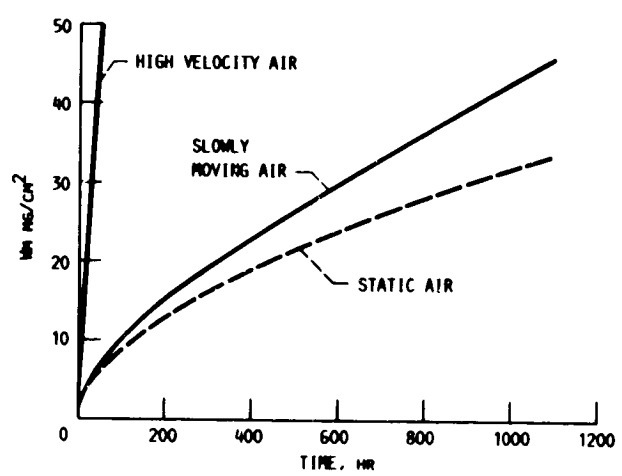

FIGURE 3. - SPECIFIC WEIGHT LOSS, W_M, OF Cr CALCULATED BY PARALINEAR ANALYSIS (COREST) FOR $AlCr_2O_3$ FORMING ALLOY Ni-40Cr AT 1473 K IN STATIC AIR, SLOWLY MOVING AIR AND HIGH VELOCITY AIR.

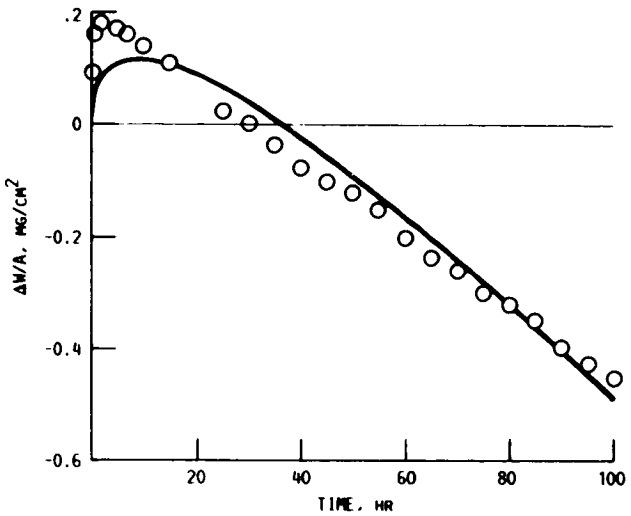

FIGURE 4. - ISOTHERMAL OXIDATION OF TD-NiCr AT 1473 K IN STATIC AIR (LOWELL, ET AL., 1971) SHOWING OBSERVED DATA AND THE CALCULATED CURVE FORM A COREST PARALINEAR ANALYSIS. k_p = .006 AND k_v = .0145.

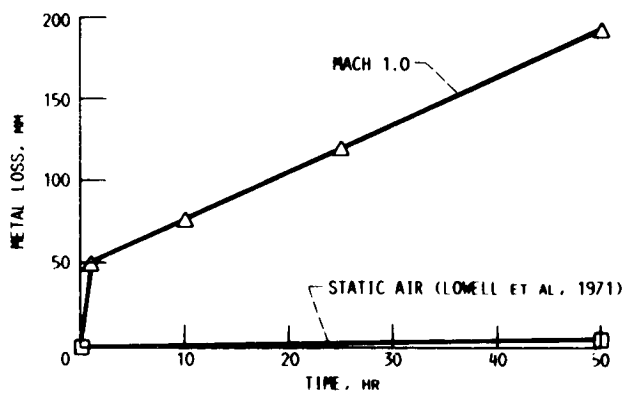

FIGURE 5. - METAL RECESSION AS A FUNCTION OF TIME DURING EXPOSURE TO MACH 1 BURNER RIG OXIDATION OF TD-NiCr AT 1473 K (LOWELL AND SANDERS, 1972).

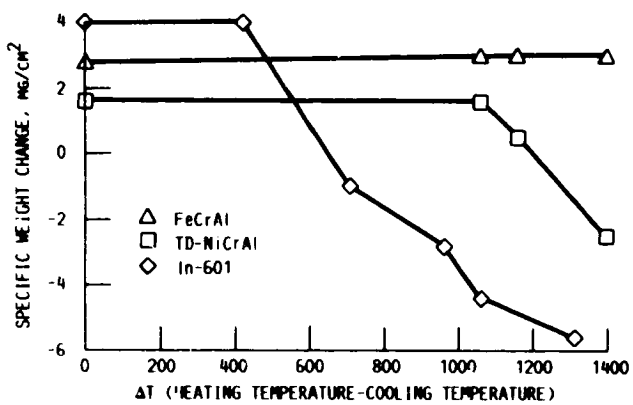

FIGURE 6. - EFFECT OF COOLING TEMPERATURE ON SCALE SPALLING DURING CYCLIC OXIDATION AT ELEVATED TEMPERATURE AFTER 200, ONE HOUR CYCLES. EACH CYCLE CONSISTS OF ONE HOUR AT TEMPERATURE FOLLOWED BY SLOW COOLING, (LOWELL AND DEADMORE, 1980).

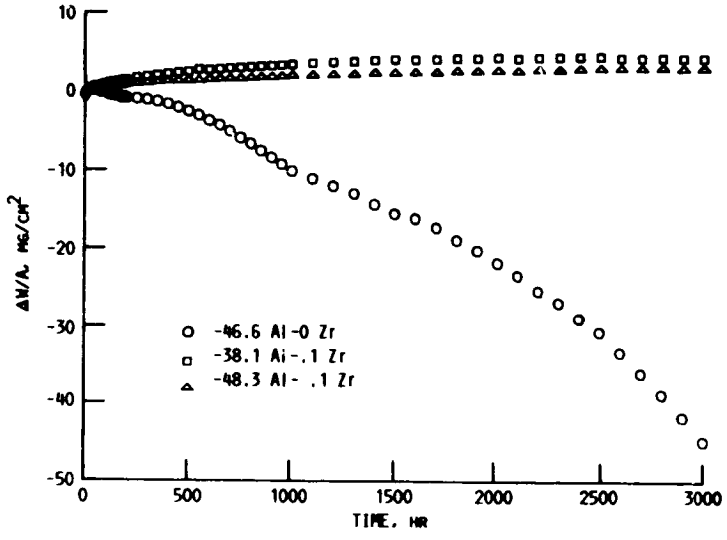

FIGURE 7. - EFFECT OF 0.1 ATOMIC PER CENT ZIRCONIUM ON THE CYCLIC OXIDATION BEHAVIOR OF BETA NiAr. SAMPLES EXPOSED FOR ONE HOUR CYCLES AT 1423 K IN STATIC AIR (BARRETT, 1988).

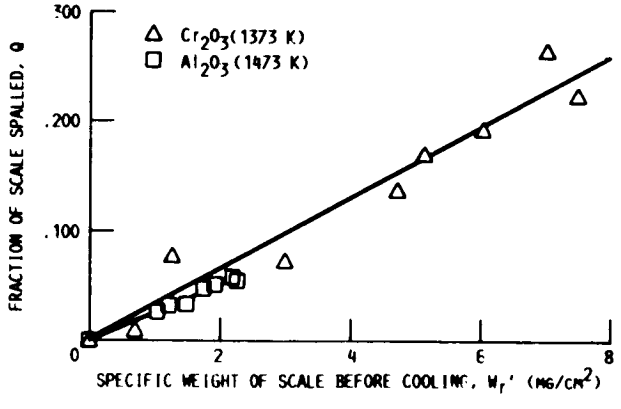

FIGURE 8. - SPALL FRACTION, Q, DEPENDENCE ON THE SPECIFIC WEIGHT OF RETAINED OXIDE PRIOR TO COOLING, W_f' FOR ALUMINA AND CHROMIA FORMING ALLOYS DURING ELEVATED TEMPERATURE OXIDATION.

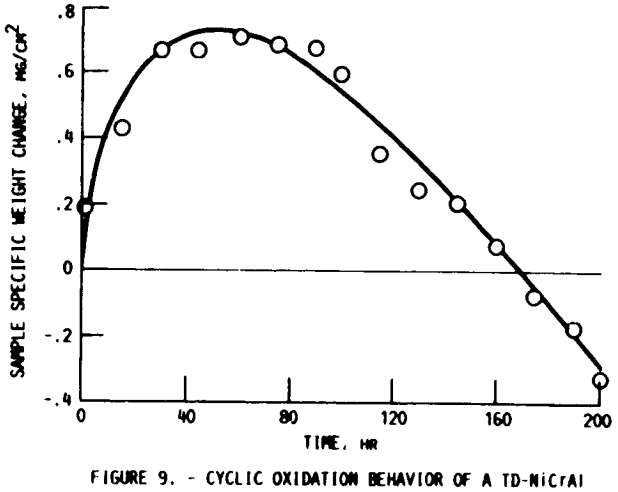

FIGURE 9. - CYCLIC OXIDATION BEHAVIOR OF A TD-NiCrAl ALLOY (UNPUBLISHED NASA LEWIS DATA) TESTED AT 1473 K FOR ONE HOUR EXPOSURE CYCLES IN STATIC AIR. OPEN SYMBOLS ARE OBSERVED DATA VALUES. THE SOLID LINE REPRESENTS A COSP MODEL COMPUTER FIT USING a = 1, K_p = .002 AND Q_0 = .003 (LOWELL, SMIALEK, AND BARRETT, 1983).

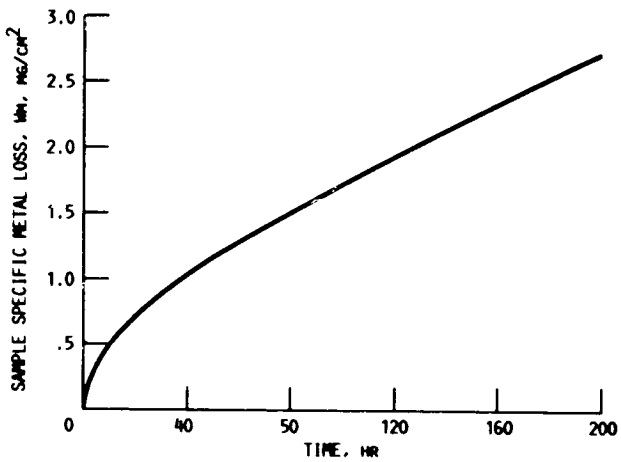

FIGURE 10. - COSP MODEL COMPUTER ESTIMATES OF THE SPECIFIC WEIGHT OF A CONSUMED, W_M, DURING THE CYCLIC OXIDATION OF A TD-NiCrAl ALLOY TESTED AT 1473 K UNDER CONDITIONS AS IN FIG. 9.

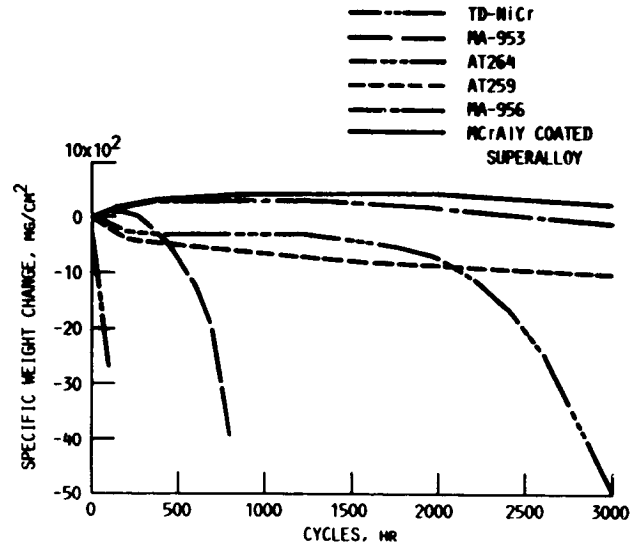

FIGURE 11. - AVERAGE WEIGHT CHANGE (DUPLICATE SPECIMENS) OF SEVERAL ODS ALLOYS AS A FUNCTION OF NUMBER OF CYCLES OF OXIDATION TESTING IN A MACH 0.3 BURNER RIG AT 1373 K. EACH CYCLE CONSISTED OF ONE HOUR AT TEMPERATURE FOLLOWED BY THREE MINUTES OF FORCED AIR COOLING (LOWELL, DEADMORE AND WHITTENBERGER, 1982).

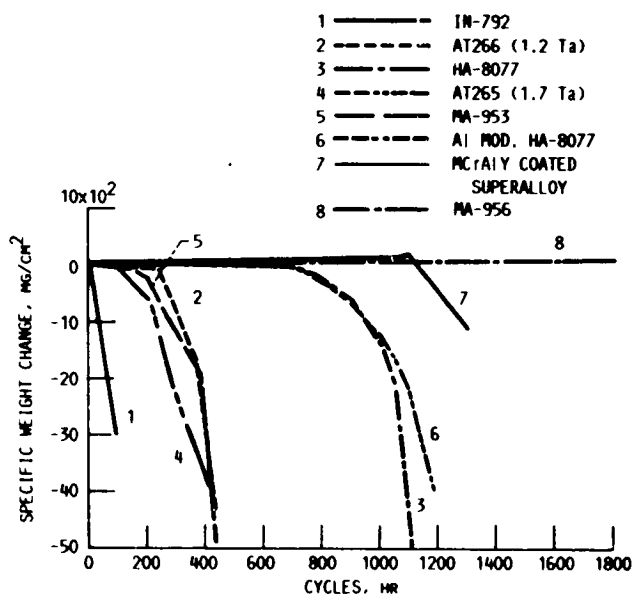

FIGURE 12. - AVERAGE WEIGHT CHANGE (DUPLICATE RUNS) OF SEVERAL ODS ALLOYS AS A FUNCTION OF CYCLIC HOT CORROSION TESTING IN A MACH 0.3 BURNER RIG AT 1173 K. THE GAS STREAM WAS DOPED WITH 5 PPM SYNTHETIC SEA SALT. EACH CYCLE CONSISTED OF ONE HOUR AT TEMPERATURE FOLLOWED BY THREE MINUTES OF FORCED AIR COOLING. THE SAMPLES WERE WASHED IN DISTILLED WATER AND DRIED BEFORE WEIGHING (LOWELL, DEADMORE AND WHITTENBERGER, 1982).

(a) MA-956, 2313 CYCLES.

(d) HDA-8077, 1119 CYCLES.

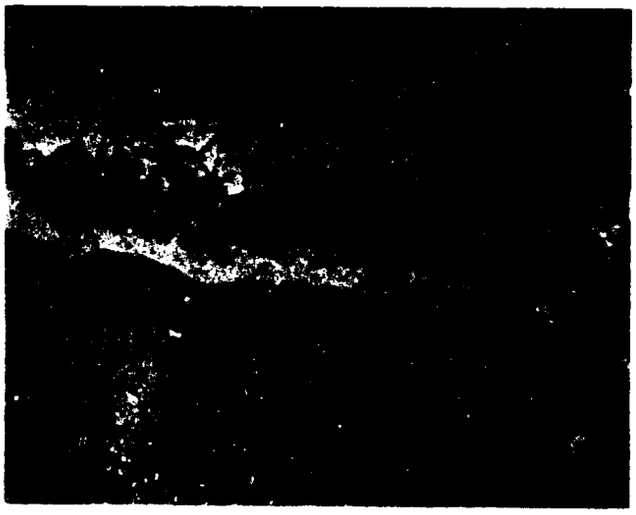

(b) STCA-266, 435 CYCLES.

(e) STCA-264, 1220 CYCLES.

(c) STCA-265, 504 CYCLES.

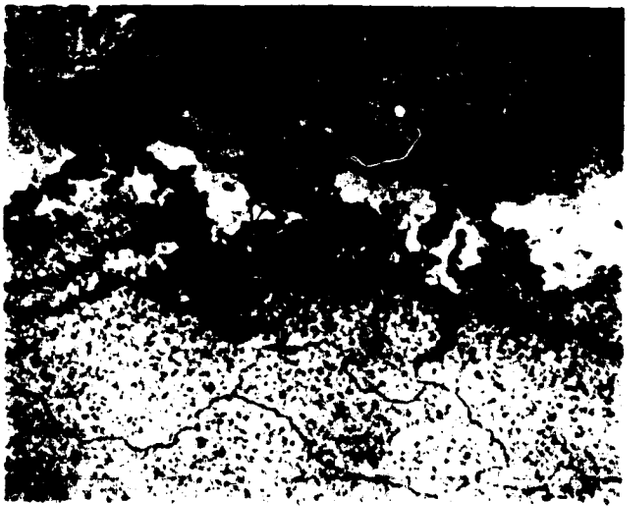

(f) NiCrAlY COATED MAR M200, 1429 CYCLES.

FIGURE 13. - TYPICAL MICROGRAPHS OF THE CORROSION ZONES OF SEVERAL ODS ALLOYS AT THE CONCLUSION OF THE TEST AS DESCRIBED IN FIG. 12. (LOWELL, DEADMORE AND WHITTENBERGER, 1982).

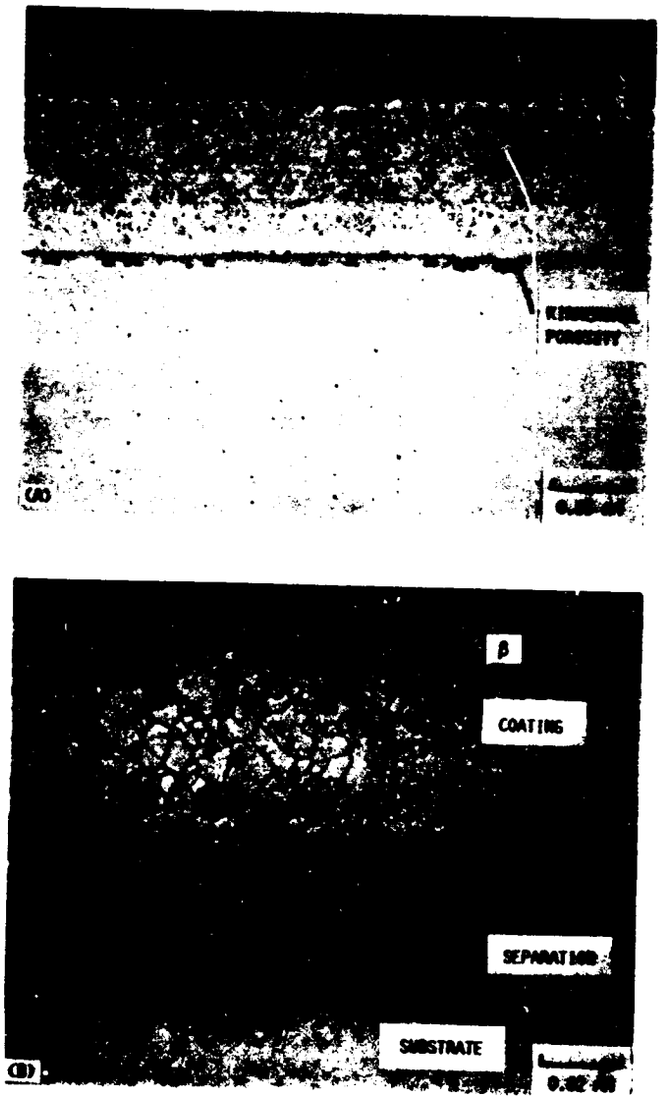

FIGURE 14. EFFECT OF HIGH TEMPERATURE EXPOSURE ON THE INTEGRITY OF THE COATING/SUBSTRATE INTERFACE OF THE COATED ODS ALLOY MA 754 (GLASGOW AND SANTORO, 1981)

NASA
National Aeronautics and Space Administration

Report Documentation Page

1. Report No.	2. Government Accession No.	3. Recipient's Catalog No.
NASA TM--102555		

4. Title and Subtitle	5. Report Date
The Oxidation and Corrosion of ODS Alloys	June 1990
	6. Performing Organization Code

7. Author(s)	8. Performing Organization Report No.
Carl E. Lowell and Charles A. Barrett	E-4030
	10. Work Unit No.
	505-63-1A

9. Performing Organization Name and Address	11. Contract or Grant No.
National Aeronautics and Space Administration Lewis Research Center Cleveland, Ohio 44135-3191	
	13. Type of Report and Period Covered
	Technical Memorandum

12. Sponsoring Agency Name and Address	14. Sponsoring Agency Code
National Aeronautics and Space Administration Washington, D.C. 20546-0001	

15. Supplementary Notes

To be published as a chapter in Handbook of Composite Materials edited by S. Ochia, Marcel Dekker, New York, New York.

16. Abstract

This paper is a review of the oxidation and hot corrosion of high temperature oxide dispersion strengthened (ODS) alloys. It classifies the environmental resistance of such alloys by oxide growth rate, oxide volatility, oxide spalling, and hot corrosion limitations. Also discussed are environmentally resistant coatings for ODS materials. The report concludes that ODS NiCrAl and FeCrAl alloys are highly oxidation and corrosion resistant and can probably be used uncoated.

17. Key Words (Suggested by Author(s))	18. Distribution Statement
Oxidation; Hot corrosion; Cyclic spalling; Coating; Dispersion strengthened alloys; High temperature; Composites	Unclassified – Unlimited Subject Category 26

19. Security Classif. (of this report)	20. Security Classif. (of this page)	21. No. of pages	22. Price*
Unclassified	Unclassified	24	A03

NASA FORM 1626 OCT 86

*For sale by the National Technical Information Service, Springfield, Virginia 22161